processes

MDPI

Article

Electrochemical Reduction Performance and Mechanism of 2,2′,4,4′-Tetrabromodiphenyl Ether (BDE-47) with Pd/Metal Foam Electrodes

Chenghao Liang [1], He Liu [2,*], Jiahao Liang [1], Xiaodong Du [1], Xueqin Tao [3] and Guining Lu [1,4,*]

[1] School of Environment and Energy, South China University of Technology, Guangzhou 510006, China; liangch@foxmail.com (C.L.); liang_jiahao@mail.tsinghua.edu.cn (J.L.); dxdon@scut.edu.cn (X.D.)
[2] South China Institute of Environmental Sciences, Guangzhou 510655, China
[3] College of Resources and Environment, Zhongkai University of Agriculture and Engineering, Guangzhou 510225, China; taoxueqin@zhku.edu.cn
[4] Key Laboratory of Pollution Control and Ecosystem Restoration in Industry Clusters, Ministry of Education, Guangzhou 510006, China
* Correspondence: liuhe@scies.org (H.L.); lutao@scut.edu.cn (G.L.)

Abstract: Polybrominated diphenyl ethers (PBDEs), a type of brominated flame retardant, are of global concern due to their environmental persistence, bioaccumulation, toxicity, and resistance to conventional remediation methods. In this study, the electrochemical reduction of 2,2′,4,4′-tetrabromodiphenyl ether (BDE-47) with Pd/Metal foam electrodes (Ni, Cu, and Ag) was investigated. The effect of Pd loadings was explored, and the results show that Pd loading enhances the debromination performance, with 15.16%Pd/Ni foam exhibiting the best efficiency, followed by 9.37%Pd/Cu and 10.26%Pd/Ag. The degradation mechanisms for Pd/Ni and Pd/Ag are primarily hydrogen atom transfer, while for Pd/Cu, electron transfer dominates. Among the reduction products, Pd/Ni foam shows the highest debromination capability. The impact of electrolytes, current intensity, and bromination degrees of PBDEs was evaluated for 15.16%Pd/Ni. The results reveal that the presence of electrolytes inhibits BDE-47 degradation; the degradation rate of BDE-47 increases with current density, peaks at 4 mA, and decreases as current rises; and 15.16%Pd/Ni foam can effectively degrade PBDEs with varying bromination levels. Additionally, cycling tests show a decrease in efficiency from 94.3% (first cycle) to 56.58% (fourth cycle), attributed to Pd loss and structural damage. The findings offer valuable insights for developing efficient, sustainable catalytic materials for the electrochemical degradation of PBDEs and other persistent organic pollutants.

Keywords: BDE-47; Pd/Metal foam electrodes; electrochemical reduction; degradation kinetics; debromination pathways; mechanism

check for updates

Academic Editor: Christos Argirusis

Received: 24 January 2025
Revised: 9 March 2025
Accepted: 11 March 2025
Published: 14 March 2025

Citation: Liang, C.; Liu, H.; Liang, J.; Du, X.; Tao, X.; Lu, G. Electrochemical Reduction Performance and Mechanism of 2,2′,4,4′-Tetrabromodiphenyl Ether (BDE-47) with Pd/Metal Foam Electrodes. *Processes* **2025**, *13*, 853. https://doi.org/10.3390/pr13030853

Copyright: © 2025 by the authors. Licensee MDPI, Basel, Switzerland. This article is an open access article distributed under the terms and conditions of the Creative Commons Attribution (CC BY) license (https://creativecommons.org/licenses/by/4.0/).

1. Introduction

Polybrominated diphenyl ethers (PBDEs) have been extensively used as cost-effective and efficient flame retardants in a wide range of applications, including electronic devices (such as circuit boards and plastic casings), building materials, household items, furniture, and transportation vehicles [1]. However, with their widespread use over the past few decades, it has become evident that PBDEs possess harmful characteristics, such as environmental persistence, bioaccumulation, and endocrine-disrupting effects [2,3]. The mass production of fire-resistant products has resulted in significant amounts of PBDEs being released into the environment, leading to serious health and ecological concerns. As a result,

PBDEs have been globally banned from production and use to mitigate their adverse impacts [4]. PBDE pollution predominantly originates from the treatment of electronic waste, and its environmental impact is challenging to mitigate within a short timeframe [5–8]. Currently, most regions worldwide lack stringent regulations to control PBDE elimination during the electronic waste dismantling process. As a result, PBDE concentrations in the environment near dismantling sites continue to rise, particularly around non-standard dismantling facilities [9–11]. In some certain electronic waste dismantling areas such as Taizhou and Guiyu, the concentration of PBDEs in the soil ranges from approximately 400 to 3000 μg/kg [10,12–15]; however, in severely contaminated regions, the concentration can escalate significantly, reaching levels as high as 10 to 300 mg/kg [16,17]. Moreover, by September 2021, 87.9% of soil samples collected from Guiyu contained PBDEs at concentrations ranging from 0.345 to 401,000 ng/kg [18]. This highlights the persistent challenge of managing PBDE pollution in electronic waste recycling areas.

Currently, the primary environmental remediation technologies for PBDEs include reduction degradation, advanced oxidation, and biodegradation. The study on the degradation of PBDEs has focused on its reductive debromination. Although advanced oxidation and biodegradation methods are capable of completely removing PBDEs, their effectiveness is generally lower than that of reduction degradation methods [19–24], primarily due to the longer oxidative degradation time required for PBDEs. Shi et al. employed a concentrated sulfuric acid/potassium permanganate system to oxidatively degrade BDE-209; while the degradation rate of BDE-209 reached 90% in the first few minutes, achieving complete removal took at least three hours [25]. Liang et al. used a thermally activated persulfate system to degrade BDE-47; under conditions of PDS:BDE-47 = 1000:1 and 60 °C, 100% degradation could be achieved within three hours [26]. However, the high temperature and persulfate dosage required make this approach less economical for practical applications. In contrast, reduction methods such as ultraviolet, zero-valent metal reduction, and TiO_2 photocatalytic reduction can achieve 100% removal of PBDEs in just a few minutes [19,27–29], demonstrating that PBDEs are more efficiently degraded through reduction processes. However, a major limitation of the current reduction methods is the incomplete debromination of PBDEs, leading to the accumulation of lower-brominated PBDE intermediates. Nevertheless, with ongoing advancements in technology, researchers have found that foam metal/electrochemical catalytic systems exhibit excellent debromination effects on PBDEs while minimizing the buildup of intermediate products, and this technology holds significant promise as an efficient method for the removal of PBDEs [20,30,31].

Electrochemical remediation is an environmentally friendly and efficient technology for pollutant removal of both heavy metals and organic compounds, offering distinct advantages for treating pollutants in complex media like wastewater and soil [30,32]. Despite electrode damage, high maintenance costs, and energy consumption, the electrochemical method's operational simplicity, automation, and compact design make it an increasingly favored approach in environmental remediation [30,32,33]. In recent years, it has become a focal point of research and application due to its ability to generate in situ hydrogen atoms with strong reducing properties, enabling the effective degradation of a wide range of pollutants [34–36]. Currently, electrochemical reduction dehalogenation commonly employs catalysts such as Pd, Pt, Rh, and Ru. These metals are favored for their excellent catalytic properties, which facilitate efficient dehalogenation processes in the treatment of halogenated pollutants. Among them, Pd has excellent catalytic properties and is often used as a catalyst to produce active species in dehalogenation reactions [22,37,38]. Numerous studies have demonstrated that the incorporation of Pd significantly enhances catalyst performance and accelerates the degradation of PBDEs. Zhuang et al. initially synthesized Pd/Fe bimetallic materials for the degradation of BDE-21, demonstrating a

degradation rate two orders of magnitude higher than that of Fe alone [39]. Subsequently, Wang et al. utilized Pd/TiO_2 under ultraviolet light to degrade BDE-47, also achieving complete degradation within approximately 10 min [40]. These studies emphasize that Pd has strong catalytic effects. In electrocatalytic hydrogenation reactions, Pd electrodes or Pd-modified electrodes notably increase the adsorption capacity of active hydrogen atoms at the electrode interface, which in turn boosts the degradation efficiency of pollutants [41–43]. Therefore, the Pd-modified electrode is likely to exhibit the capability to efficiently remove PBDEs while minimizing the generation and accumulation of lower brominated PBDEs.

Overall, this study aims to explore the electrochemical reduction and degradation removal performance of BDE-47 using Pd-modified foam metals with different electrochemical properties, including Ni, Cu, and Ag foam. Pd is chemically deposited onto these foam metals to create a variety of Pd-loaded electrode materials. BDE-47, a frequently detected and highly toxic environmental contaminant, is selected as a model compound for investigation. This study explores the degradation kinetics of BDE-47 involving Pd/Ni, Pd/Cu, and Pd/ Ag foam, and then analyzes the reduction products of BDE-47 to identify the dominant reaction mechanisms involved in its degradation with different foam materials. The electrode material with the most effective degradation performance is further examined to assess the impact of various environmental factors on its performance. Additionally, the cyclic stability and surface morphology changes of the material are investigated to better examine the foam material's long-term performance. The overall goal of this research is to develop a clean and efficient method for the removal of PBDEs based on electrochemical catalysis, providing new insights into the degradation of halogenated organic pollutants.

2. Materials and Methods

2.1. Chemicals

The authentic PBDE standards of 4-mono-PBDE (BDE-3), 4,4′-di-PBDE (BDE-15), 2,4,4′-tri-PBDE (BDE-28), 2,2′,4,4′-tetra-PBDE (BDE-47), 2,2′,4,4′,5-penta-PBDE (BDE-99), 2,2′,4,4′,6-penta-PBDE (BDE-100), 2,2′,4,4′,5,5′-hexa-PBDE (BDE-153), 2,2′,4,4′,5,6′-hexa-PBDE (BDE-154), and 2,2′,3,4,4′,5′,6-tetra-PBDE (BDE-183) were purchased from AccuStandard Inc., New Haven, CT, USA. The internal standard of 2,3,4,5-tetrachlorinated biphenyl (PCB-61) was purchased from ANPEL Laboratory Technologies Inc., Shanghai. The purities of all of the above authentic standards were greater than 99%. The Ni foam, Cu foam, and Ag foam were purchased from Yizhongtian New Material Co. (Kunshan, China). $PdNa_2Cl_4$ was purchased from Adamas Co., Ltd. (Shanghai, China). HPLC-grade solvents of methanol, acetonitrile, hexane, and acetone were purchased from Aladdin Bio-Chem Technology Co., Ltd. (Shanghai, China). The ultra-pure water was acquired from Millipore milli-Q system (Burlington, MA, USA).

2.2. Preparation of Metal Foam Electrodes

2.2.1. Pre-Treatment of Metal Foam Electrodes

The metal foam electrodes were first cut into dimensions of 20 × 50 mm (length × width). They were then immersed in acetone and sonicated for 60 min to remove all the possible organic contaminants from the surface. Next, the electrodes were washed with oxygen-free water and placed into an 80 g/L sulfuric acid solution. The electrodes were sonicated for 60 to 120 s to remove the oxide layer from the metal surface. After sonication, the electrodes were immediately rinsed with oxygen-free water. Finally, the metal foam electrodes were immersed in methanol and stored for future use.

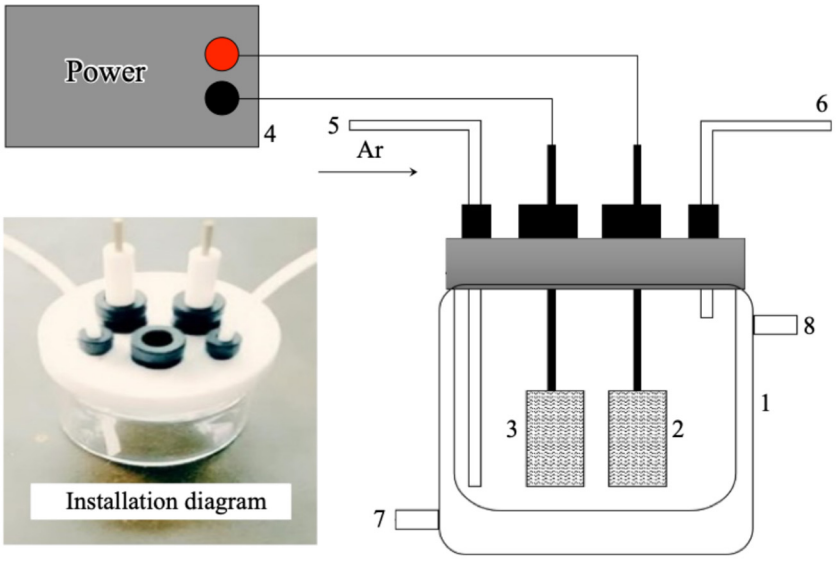
2.2.2. Synthesis of Pd-Modified Metal Foam Electrodes

Based on the metal activity series, Pd^{4+} ions in the Na_2PdCl_4 solution were chemically reduced and spontaneously deposited onto the surface of the foam metal electrode, yielding the Pd-modified foam electrode (Pd/Metal foam) material required for this study. A total of three electrode materials, Pd/Ni foam, Pd/Cu foam, and Pd/Ag foam, were prepared by loading Pd particles onto Ni foam, Cu foam, and Ag foam by chemical deposition. Different volumes of 10 mM Na_2PdCl_4 solution were used to obtain the electrodes with different Pd particle loadings.

For synthesizing the Pd-modified metal foam electrodes, the pre-formulated 10 mM Na_2PdCl_4 was added to the pre-treated foam electrodes and adjusted to a total volume of 40 mL using oxygen-free water. Several pieces of foam metal with specific mass were placed into the 50 mL centrifuge tubes. Then, the tubes were vortexed and shaken at 2000 rpm for 1 h. Afterward, the foam materials were taken out, rinsed with oxygen-free water under slow flow, and vacuum freeze-dried for 24 h. Following the drying process, the samples were placed in drying dishes for later use. The theoretical Pd-loading ratios of Ni foam, Cu foam, and Ag foam electrodes are depicted in Table S1.

2.3. Degradation Procedures

The basic electrolyte for BDE-47 degradation experiments was prepared by mixing methanol and oxygen-free water in a 6:4 ratio, which contained 0.05 mol/L H_2SO_4 and 20 ppm of BDE-47. A cylindrical single-cell glass electrolyzer was used as the reaction vessel (Figure 1). At the beginning, 50 mL of the prepared electrolyte was added to the reactor, with rotor stirring set at 300 rpm. The anode was a platinum sheet electrode (10 × 10 × 0.1 mm) while the cathode consisted of a Pd/Metal foam electrode. The electrolysis was initiated by energizing the electrodes, and the reaction time was simultaneously recorded. Samples were taken at reaction intervals of 0, 5, 10, 20, 30, 45, 60, and 90 min. For each sample, 1 mL was transferred into a chromatographic vial for kinetic analysis using HPLC. An additional 1 mL was transferred into a 4 mL vial, and 1 mL of hexane extract (0.100 mg L^{-1} PCB-61 as the internal standard) was added. The mixture was shaken with a vortex shaker for 20 min to facilitate extraction. Finally, approximately 1 mL of the organic solvent containing possible degradation products was transferred to a new vial for GC/MS analysis.



1. Electrolytic cell; 2. Anode; 3. Cathode; 4. Power supply or electrochemical workstation; 5. Ar inlet; 6. Ar outlet; 7. Water inlet; 8. Water outlet

Figure 1. Schematic diagram of the cylindrical single-cell glass electrolyzer.

2.4. Analytic Methods

High-Performance Liquid Chromatography (HPLC) was employed for the quantitative analysis of PBDEs. The analysis was carried out using a Phenomenex Luna C18 reverse-phase separation column (San Diego, CA, USA) with a flow rate of 1 mL/min. The mobile phase consisted of 15% water and 85% acetonitrile, and the column was maintained at a temperature of 40 °C.

Qualitative analysis of the debromination products of BDE-47 was performed with a Thermo Trace GC Ultra gas chromatography coupled to a DSQ II mass spectrometer detector (Thermo-Electron Corporation, Waltham, MA, USA). The mass spectrometer was equipped with an electron ionization (EI) source. An Agilent DB-5MS capillary column (30 m × 0.25 mm × 0.25 μm) (Santa Clara, CA, USA) was used for compound separation. The carrier gas of helium was set at a constant flow of 1 mL/min, and the temperature of the inlet was set at 280 °C with the splitless mode. The injection volume was set to 1 μL. The oven temperature was initiated at 120 °C for 1 min, then increased to 290 °C at a rate of 20 °C/min, then held for 2 min. All the samples were analyzed in both full scan mode and selective ion monitoring (SIM) mode. All the results were processed by Xcalibur software (Version 2.2.0).

2.5. Characterization of Pd/Metal Foam

The Zeiss Scanning Electron Microscopy (SEM) couped to Energy Dispersive X-ray Spectroscopy (EDS) (Oberkochen, Germany) were employed to visualize the microscopic surface properties of the Pd/Metal foam. Before SEM and EDS analysis, the samples were cut into appropriate sizes, vacuum-dried, and then characterized using SEM-EDS. The SEM was operated at an accelerating voltage of 10 kV, with a magnification range of 50–5000× and a working distance of 10 mm. For EDS analysis, the accelerating voltage was set to 5 kV, with a counting time of 100 s. The EDS measurements were conducted using a silicon drift detector to analyze the elemental composition of the materials.

3. Results and Discussion

3.1. Kinetics

In this study, we selected BDE-47 as a model compound, as it is the most toxic and frequently detected PBDE congeners in the environment. Five Pd/Ni foam electrodes with different Pd loading contents (2.12%, 4.17%, 8.07%, 15.16%, and 21.44%) were chosen for the degradation experiments. As illustrated in Figure 2a,b, increasing the Pd loading significantly enhances the catalytic degradation ability of the Ni foam electrode. With no Pd loaded, the Ni foam electrode achieved only a 9.5% degradation rate of BDE-47 over 90 min without current. In contrast, the Ni foam electrode achieved a 23.3% degradation rate of BDE-47 over 90 min with current. The involvement of Pd significantly enhanced the degradation of BDE-47, with 2.39%Pd/Ni foam exhibiting a 42.24% degradation rate within just 30 min. As the Pd loading increased, the degradation effect initially increased, peaking at 16.39%Pd/Ni foam, and then began to decrease at higher loadings. In addition, for Pd/Ni foam with Pd loading less than 16.39%, the reaction reached equilibrium in approximately 30 min. However, when the Pd loading was greater than 16.39%, the degradation rate slowed down, but the degradation rate still reached 90% within 90 min. The first-order kinetic fitting results revealed the BDE-47 degradation rates under different Pd loading amounts: 1.384, 1.964, 3.128, 5.644, and 2.291 h^{-1}, respectively. These results highlight the significant influence of Pd loading on the catalytic degradation performance of the Ni foam electrodes. It is noteworthy that during the degradation of BDE-47 with Pd/Ni foam, rapid degradation was observed at the beginning of the reaction, followed by a slower degradation equilibrium stage (Figure 3a–c). Further analysis of the equilibrium stage

revealed that the degradation rate of BDE-47 during this stage was slow and comparable to that of Ni foam without Pd. This observation suggests that Pd may be consumed during the degradation process, leading to a subsequent equilibrium state in the reaction.

Although Pd/Cu bimetallic catalysts are extensively utilized in the catalytic degradation of halogen-containing organic compounds, their application in the form of Pd/Cu foam electrodes for the electrocatalytic degradation of halogenated organic pollutants remains limited [44]. Pd/Cu foam electrodes with Pd loadings of 1.25%, 2.48%, 4.86%, 7.16%, and 9.37% were prepared and evaluated. As illustrated in Figures 2c,d and 3d, unmodified Cu foam exhibited almost no degradation effect on BDE-47 without current. However, with current, the removal rate of BDE-47 reached 23.7% within 90 min, slightly higher than that of Ni foam (23.3%). When Pd was loaded onto Cu foam, the degradation efficiency of BDE-47 for 1.25%Pd/Cu, 2.48%Pd/Cu, and 4.86%Pd/Cu foams was similar to that of unmodified Cu foam. The reaction rates suggested that the addition of Pd slightly inhibited the degradation of BDE-47 at lower loading levels. However, as the Pd loading increased, the degradation efficiency improved progressively. When Pd was loaded onto Cu foam, the degradation efficiency of BDE-47 for 1.25%Pd/Cu, 2.48%Pd/Cu, and 4.86%Pd/Cu foams was similar to that of unmodified Cu foam. The reaction rates suggested that the addition of Pd slightly inhibited the degradation of BDE-47 at lower loading levels. Furthermore, the degradation behavior of BDE-47 using all Pd/Cu foam electrodes followed a first-order kinetic process, and unlike Pd/Ni foam, no equilibrium stage was observed during the reaction. This indicates consistent and sustained degradation activity throughout the reaction period.

Pd/Ag materials have been extensively studied in the field of electrocatalysis [45–47]. However, their degradation performance and mechanism for brominated organic compounds, such as PBDEs, have rarely been explored. Ag foam electrodes with Pd loadings of 1.36%, 2.70%, 5.30%, 7.83%, and 10.26% were prepared and tested for their degradation performance. As shown in Figures 2e,f and 3e, unmodified Ag foam exhibited no degradation effect on BDE-47 in the absence of current. When powered, the removal rate of BDE-47 by Ag foam reached 18.2% within 90 min, which is lower than the corresponding rates achieved by Pd/Ni foam and Pd/Cu foam under similar conditions. The addition of Pd onto Ag foam promoted the degradation of BDE-47, with the degradation efficiency positively correlated with the Pd loading amount. However, compared to Pd/Ni foam and Pd/Cu foam, the degradation rate of BDE-47 under 10.26%Pd/Ag foam was only 74.8% in 90 min, indicating that the enhancement provided by Pd on Ag foam was limited. This limitation may be attributed to the inherent physical and chemical properties of Ag, which are less conducive to catalytic performance compared to Ni or Cu. Similar to Pd/Cu foam, the degradation behavior of BDE-47 using Pd/Ag foam electrodes followed a first-order kinetic process, with no equilibrium stage observed throughout the reaction.

In summary, Pd loading was found to have the most significant effect on the catalytic performance of Ni foam, although the degradation rate of BDE-47 decreased over time due to the loss of Pd on the Ni foam surface. In contrast, Pd loading had a minimal effect on Cu foam at low levels but significantly improved the degradation performance of BDE-47 at higher loadings. On the other hand, Pd loading on Ag foam showed only limited improvement in degradation performance, even at high loadings, likely due to the inherent properties of Ag foam. These results highlight that the catalytic enhancement effect of Pd is material-dependent, with Ni foam being the most favorable substrate for BDE-47 degradation, followed by Cu foam, while Ag foam showed the least improvement.

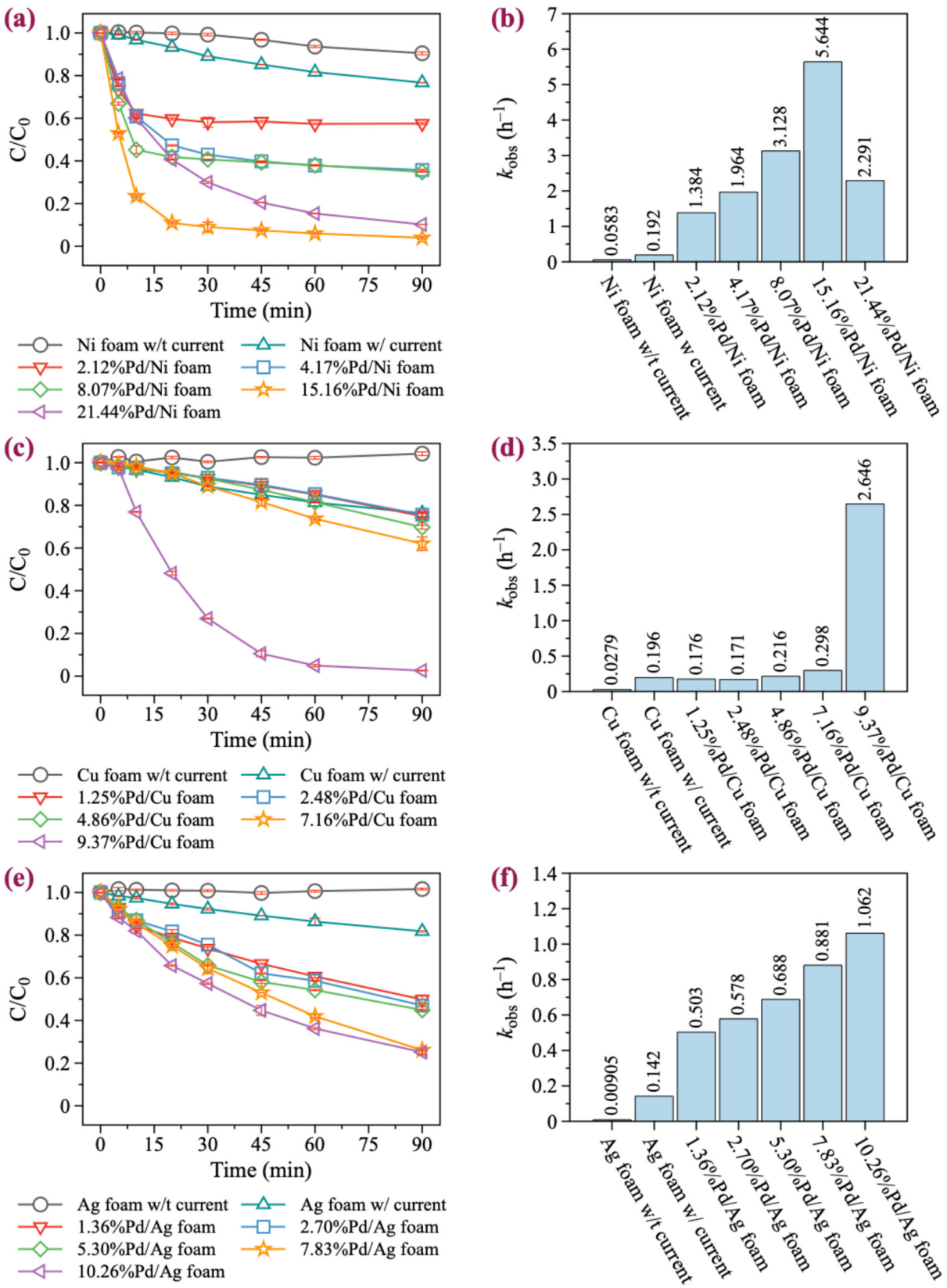


Figure 2. Degradation kinetics of BDE-47. (**a**,**c**,**e**) The degradation kinetics of BDE-47 with Pd/Ni, Pd/Cu, and Pd/Ag foam, respectively. (**b**,**d**,**f**) The kobs of BDE-47 with Pd/Ni, Pd/Cu, and Pd/Ag foam, respectively.

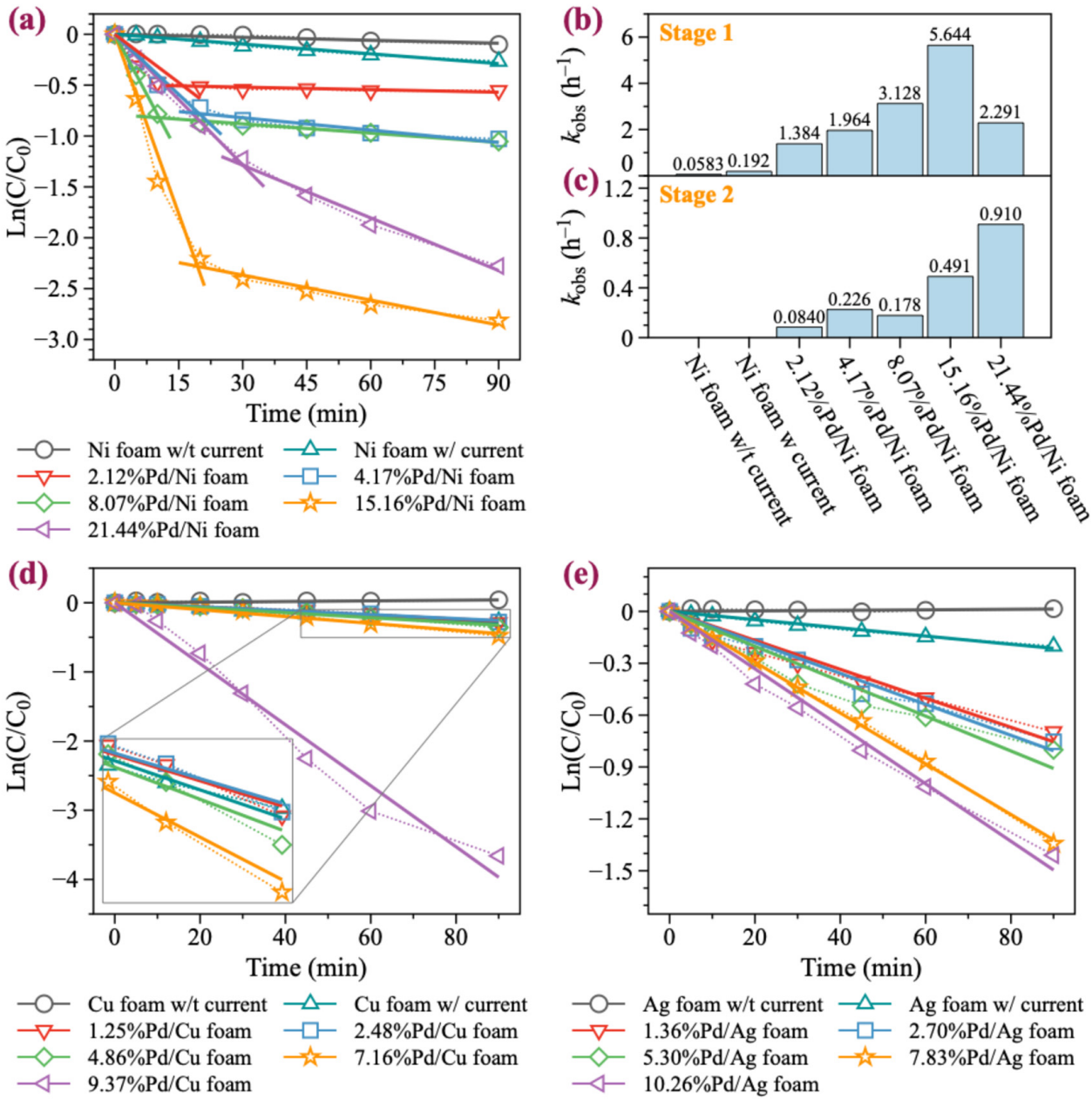


Figure 3. First-order kinetic fittings of BDE-47 with Pd/Ni, Pd/Cu, and Pd/Ag foam. (**a**) Fitted lines of BDE-47's degradation with Pd/Ni foam. (**b**,**c**) Fitted k_{obs} of BDE-47 with Pd/Ni foam at different degradation stages. (**d**) Fitted lines of BDE-47's degradation with Pd/Cu foam. (**e**) Fitted lines of BDE-47's degradation with Pd/Ag foam.

3.2. Degradation Products and Mechanisms

We further detected and analyzed the degradation products of BDE-47 under Pd/Ni, Pd/Cu, and Pd/Ag conditions to elucidate the degradation mechanism of BDE-47 on different electrode materials. The reductive debromination of polybrominated diphenyl ethers (PBDEs) primarily involves two mechanisms: the active hydrogen atom transfer mechanism and the electron transfer mechanism. By comparing the types and abundances of primary debromination products, the dominant degradation mechanism in the current system was inferred. BDE-47 has two primary debromination products: BDE-28, formed by the removal of an ortho-C/Br bond, and BDE-17, formed by the removal of a para-C/Br bond. The complete degradation pathway of BDE-47 is shown in Figure S1.

GC/MS analysis revealed various reduction products of BDE-47. Under Pd/Ni foam conditions, no significant debromination products were detected with low Pd loading (e.g., 2.12%Pd/Ni foam) (Figure S2). However, as the Pd loading increased, the abundance of products with different bromination levels gradually rose, with lower brominated PBDEs becoming the dominant products. This demonstrates that Pd/Ni foam exhibits an effective debromination capability for BDE-47. In particular, under 15.16%Pd/Ni foam, the abundance of debromination products was significant, with BDE-3 and diphenyl ether (DE) being the major products (Figure 4a). Nevertheless, analyzing the formation of BDE-28 and BDE-17 revealed that the abundance of BDE-17 consistently exceeded that of BDE-28, indicating that the degradation of BDE-47 under Pd/Ni foam is primarily governed by the active hydrogen atom transfer mechanism. Summarizing the product generation under Pd/Ni foam conditions, the reductive degradation pathway of BDE-47 proceeds as follows: BDE-47 → BDE-17 → BDE-8 → BDE-3 → DE.

For Pd/Cu foam, the amount of BDE-47 reduction products was found to be low under low Pd loading conditions (1.25%, 2.48%, 4.86%), with minimal difference in the abundances of BDE-17 and BDE-28 (Figure S3). However, as the Pd loading increased to 7.16%, the abundance of BDE-28 slightly exceeded that of BDE-17. At the highest Pd loading of 9.37% (Figure 4b), the abundance of BDE-28 significantly increased, with a notable rise in the amount of BDE-15. These observations strongly suggest that the reductive degradation of BDE-47 under Pd/Cu foam conditions is predominantly governed by the electron transfer mechanism. At lower Pd loading levels, however, neither the active hydrogen atom transfer mechanism nor the electron transfer mechanism contributed significantly to the degradation of BDE-47. This lack of dominance resulted in minimal differences in the abundances of BDE-28 and BDE-17, and the competition between these two mechanisms likely explains the lower degradation rates of BDE-47 observed under low Pd loading. Additionally, no formation of lower brominated PBDEs was detected in this system, indicating a limited debromination effect of Pd/Cu foam on BDE-47. In general, under Pd/Cu foam conditions, the reductive degradation pathway of BDE-47 can be described as BDE-47 → BDE-28 → BDE-15. This pathway, coupled with the absence of further debromination products, highlights the limited degradation capability of Pd/Cu foam, especially at lower Pd loadings.

For Pd/Ag foam, abundant reduction products of BDE-47 were observed under all Pd loading conditions (Figure S4). Further analysis revealed that the abundance of BDE-17 was consistently higher than that of BDE-28 (Figure 4c), suggesting that the degradation of BDE-47 under Pd/Ag foam conditions is predominantly governed by the active hydrogen atom transfer mechanism. Additionally, significant amounts of lower brominated PBDEs were detected under various Pd loading conditions, indicating that Pd/Ag foam has good debromination efficiency for BDE-47. However, due to its relatively slower degradation rate for BDE-47, its debromination effect is not as pronounced as that of Pd/Ni foam. It is worth noting that due to chromatographic limitations, we were unable to completely separate BDE-4 and BDE-7. However, based on the observed product distribution and degradation pathways, BDE-7 is considered to be the more likely product. In conclusion, the reductive degradation pathway of BDE-47 under Pd/Ag foam conditions can be summarized as BDE-47 → BDE-17 → BDE-7 → BDE-3 → DE. Although Pd/Ag foam shows good debromination performance, its overall efficiency is limited by its slower degradation rate compared to Pd/Ni foam.

Overall, Pd/Ni foam demonstrated the highest debromination efficiency and fastest degradation rate, driven by the active hydrogen atom transfer mechanism. Pd/Cu foam showed limited debromination but had an electron transfer mechanism that dominated at higher loadings, leading to efficient degradation. Pd/Ag foam achieved good debromina-

tion but was constrained by slower degradation rates, even though it produced abundant lower brominated PBDEs. The results highlight the role of Pd-loaded-foam electrodes in PBDEs' degradation performance and mechanism.

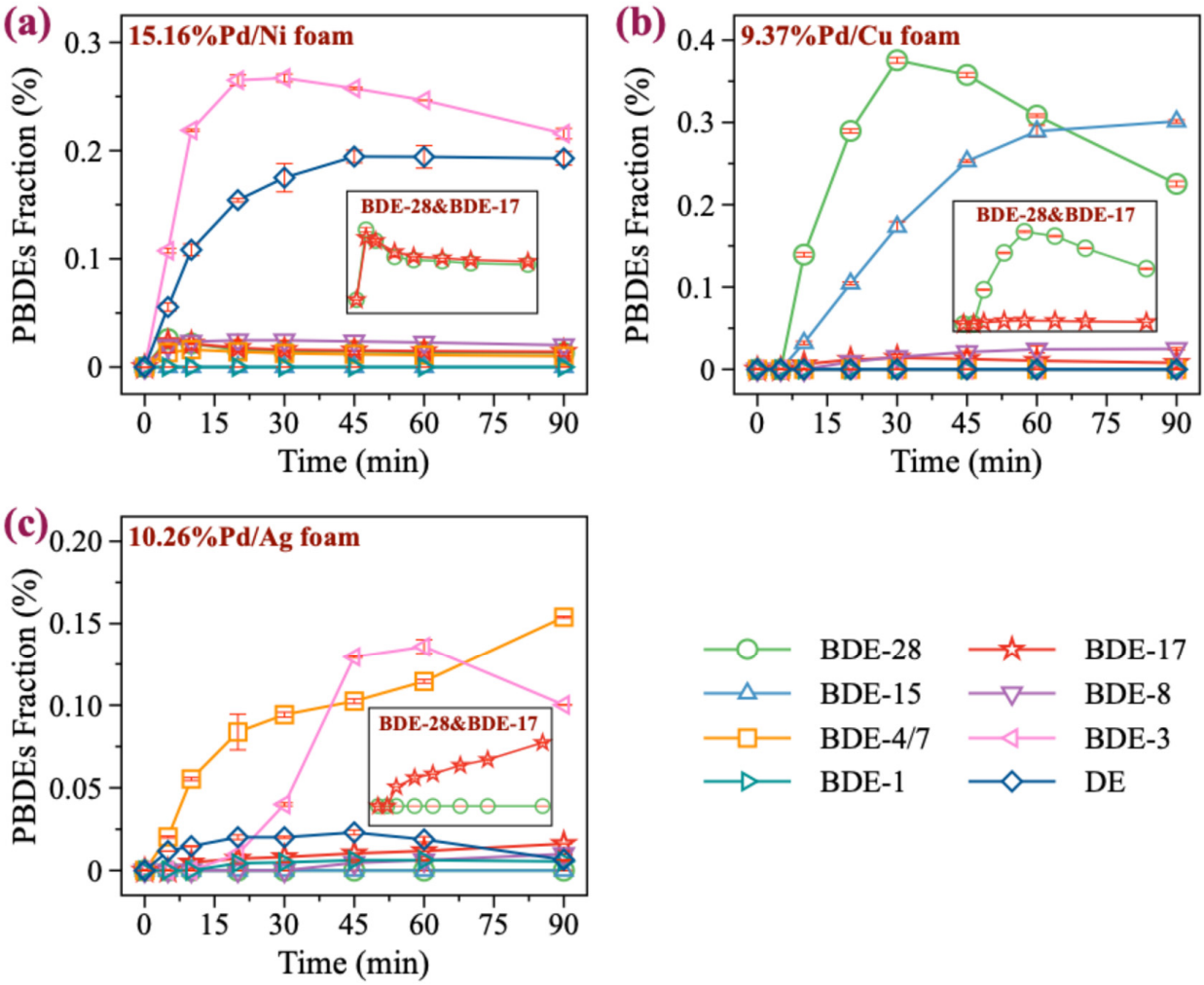


Figure 4. Production of the debromination products from BDE-47. (**a**–**c**) The products of BDE-47 in 15.16%Pd/Ni, 9.37%Pd/Cu, 10.26%Pd/Ag, respectively.

3.3. Influencing Factors

3.3.1. Electrolytes

The microscopic chemical properties of electrolytes play a crucial role in influencing electrochemical processes. So, we investigated the effects of four common electrolytes (NaCl, Na_2SO_4, KCl, and K_2SO_4) on the electrochemical reduction debromination of BDE-47 using the Pd/Ni foam electrode with 15.16%Pd loading. The electrolyte concentration was 0.05 mol/L. The experimental results showed that the debromination rates of BDE-47 were 71.03% for NaCl, 83.53% for Na_2SO_4, 74.36% for KCl, and 87.36% for K_2SO_4 (Figure 5). But compared to the previous results, it is obvious that all four electrolytes strongly inhibited the degradation of BDE-47 to varying degrees. For Cl salts (NaCl and KCl), the initial inhibition was attributed to the high concentration of Cl^- ions competing with BDE-47 for active hydrogen generated in the system, thereby reducing the availability of hydrogen for debromination. However, as the reaction progressed, Cl^- ions were gradually consumed, allowing for the degradation rate of BDE-47 to increase in the later stages. However, for SO_4^{2-} salts (Na_2SO_4 and K_2SO_4), an initial inhibition period was observed during the first 60 min of the reaction. This was likely due to the high concentration of SO_4^{2-} ions

temporarily inhibiting the activity of the Pd/Ni foam electrode. However, as the reaction continued, the Pd/Ni foam electrode became more active with continuous current, resulting in rapid degradation of BDE-47 after the inhibition period. Moreover, the presence of K^+ ions slightly improved the debromination performance compared to Na^+ ions under similar conditions. This is likely due to K^+ ions enhancing current conduction efficiency in the reaction system.

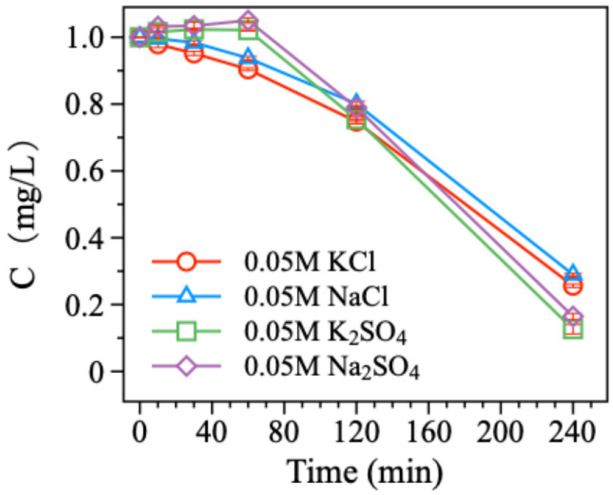


Figure 5. Degradation of BDE-47 in different electrolytes.

3.3.2. Current Intensity

The degradation performance of BDE-47 under different current intensities was explored using the 15.16%Pd/Ni foam electrode (Figure 6). The tested current intensities were 0, 0.5, 1.0, 2.0, 3.0, 4.0, 6.0, 8.0, and 10.0 mA. The results showed that the 15.16%Pd/Ni foam electrode could degrade BDE-47 without an applied current, but the degradation efficiency was relatively low, achieving only a 21.6% degradation rate after 90 min. As the current intensity increased, the degradation rate of BDE-47 improved, reaching the highest efficiency at 4.0 mA. These results demonstrate that the external electric field significantly enhances the catalytic degradation performance of the Pd/Ni foam electrode. However, at current intensities above 4.0 mA, the degradation efficiency began to decline, with a more pronounced inhibitory effect observed as the current intensity further increased. This decline in degradation performance at higher current intensities is likely due to the rapid loss of Pd on the surface of the Pd/Ni foam during the catalytic process, which hinders the continued degradation of BDE-47. These results suggest that the external electric field is critical for enhancing degradation, while excessive current intensity accelerates the depletion of Pd, thereby reducing the electrode's catalytic efficiency. Herein, we infer that optimizing the current intensity and controlling Pd loss on the surface of the Pd/Ni foam are essential for maintaining high degradation efficiency and prolonging the electrode's catalytic performance during the degradation of PBDEs.

3.3.3. PBDEs with Different Bromination Degrees

The number of aromatic rings, the benzene ring configuration, and the C/X bond position of aromatic bromides are the basic factors that affect the reaction [48,49]. The degradation performance of 15.16%Pd/Ni foam on PBDEs with varying degrees of bromine atom substitution was investigated, using nine representative PBDE monomers (BDE-183, BDE-154, BDE-153, BDE-100, BDE-99, BDE-47, BDE-28, BDE-15, and BDE-3) commonly found in commercial pentabromodiphenyl ether mixtures [50–52]. The results demonstrated that all nine PBDEs can be rapidly degraded within 90 min of reaction time, achieving degradation rates of over 80% (Figure 7). The degradation kinetics indicate that the

catalytic degradation of PBDEs by Pd/Ni foam is not significantly affected by the degree of bromine atom substitution, suggesting that the number of bromine atoms in PBDEs does not play a limiting role in the reduction debromination process. This highlights the universality of the Pd/Ni foam electrode in effectively degrading PBDEs across a broad range of bromination levels.

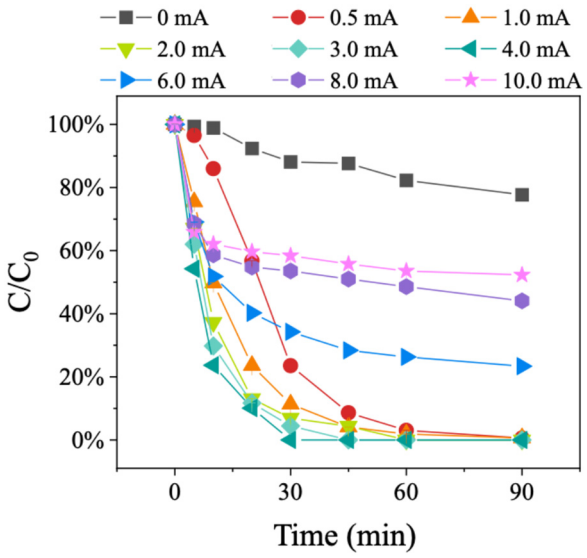


Figure 6. Degradation of BDE-47 in different current intensities.

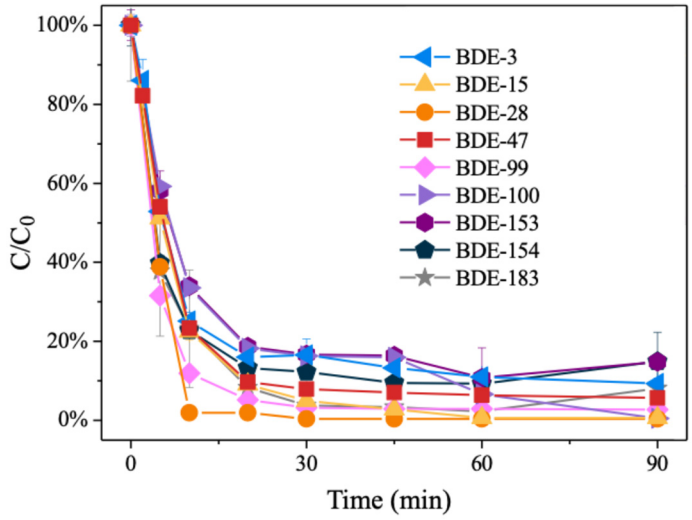


Figure 7. The degradation kinetics of PBDEs of different bromination levels with 15.16%Pd/Ni foam.

3.4. SEM Characterization

The 15.16%Pd/Ni foam electrode was selected for characterization using SEM and EDS to observe morphological changes before and after the 90 min reaction (Figure 8). The initial Ni foam exhibits a typical flower-like microstructure (Figure 8a). After Pd loading, the overall size of the "nickel flower" remains unchanged (Figure 8b); however, the edges of the flower become blunter and the "petals" appear to be much rougher. During the reaction, the surface morphology of the Pd/Ni foam undergoes significant changes. Initially (0 min), the structure maintains its flower-like shape, but as the reaction progresses, it first transforms into a "flower ball" (30 min) (Figure 8c) and ultimately into a granular structure (90 min) (Figure 8d). This morphological evolution is attributed to the electrochemical reaction occurring on the electrode surface, where continuous erosion and structural remodeling

take place. The SEM images also further explain why the degradation rate of BDE-47 appears to be much slower as the reaction proceeds.

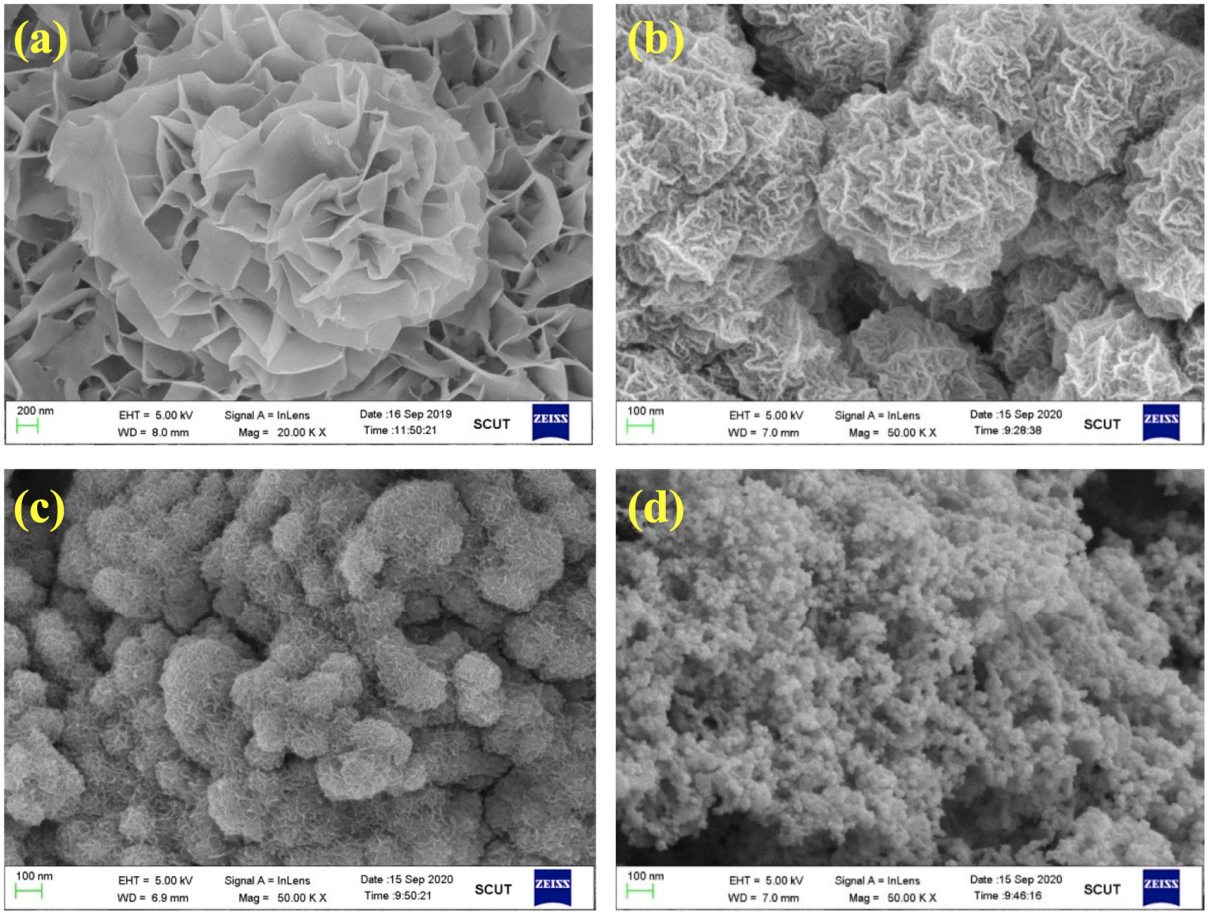


Figure 8. SEM of 15.16%Pd/Ni foam before and after a reaction. (**a**) The Ni foam without Pd loading. (**b**) The 15.16%Pd/Ni foam before reaction. (**c**) The 15.16%Pd/Ni foam after a 30 min reaction. (**d**) The 15.16%Pd/Ni foam after a 90 min reaction.

3.5. Electrode Cycling Performance

The stability of the electrode is crucial for its practical application. So, the 15.16%Pd/Ni foam electrode was further evaluated through cycling experiments to assess its performance. As shown in Figure 9, the degradation efficiency of BDE-47 decreased progressively over four consecutive cycles. Visible corrosion and slight damage to the electrode were observed, along with black particle shedding into the solution. In terms of kinetic performance, the system achieved optimal degradation in the first cycle, achieving a 94.3% removal rate of BDE-47 within 90 min. However, with subsequent cycles, the degradation efficiency declined to 64.26%, 58.74%, and 56.58% in the second, third, and fourth cycles, respectively. SEM analysis revealed significant surface corrosion and material shedding after the four cycles, with substantial Pd loss from the surface of the Pd/Ni foam (Figure 10). It is speculated that the reason for the corrosion and shedding of Pd/Ni foam may be the embrittlement and fracture of the material caused by the diffusion of hydrogen atoms in the metal phase. As Pd has a higher capacity for hydrogen storage compared to Ni, the repeated absorption and release of hydrogen atoms lead to the peeling and fragmentation of Pd. To enhance the long-term stability of Pd/Ni foam electrodes, it is essential to develop methods for securely anchoring Pd to the substrate and to minimize corrosion caused by overly acidic electrolytes when using Ni foam as the cathode.

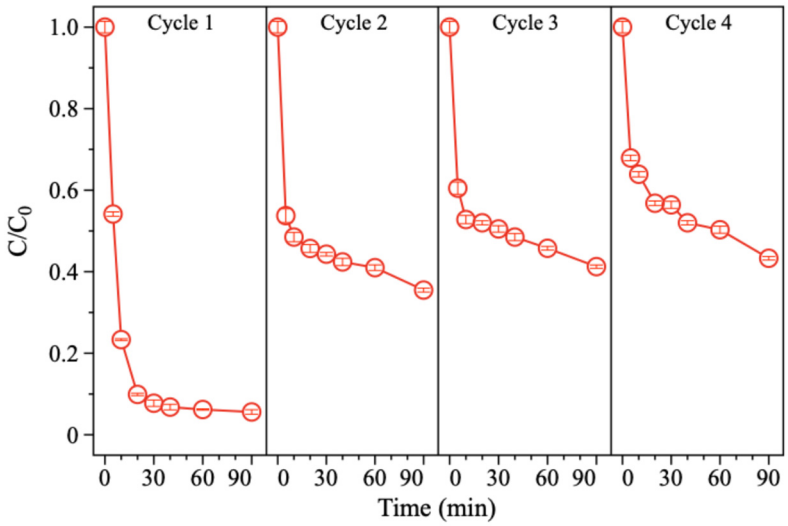


Figure 9. Performance of 15.16%Pd/Ni foam in degrading BDE-47 in four repetitive experiments.

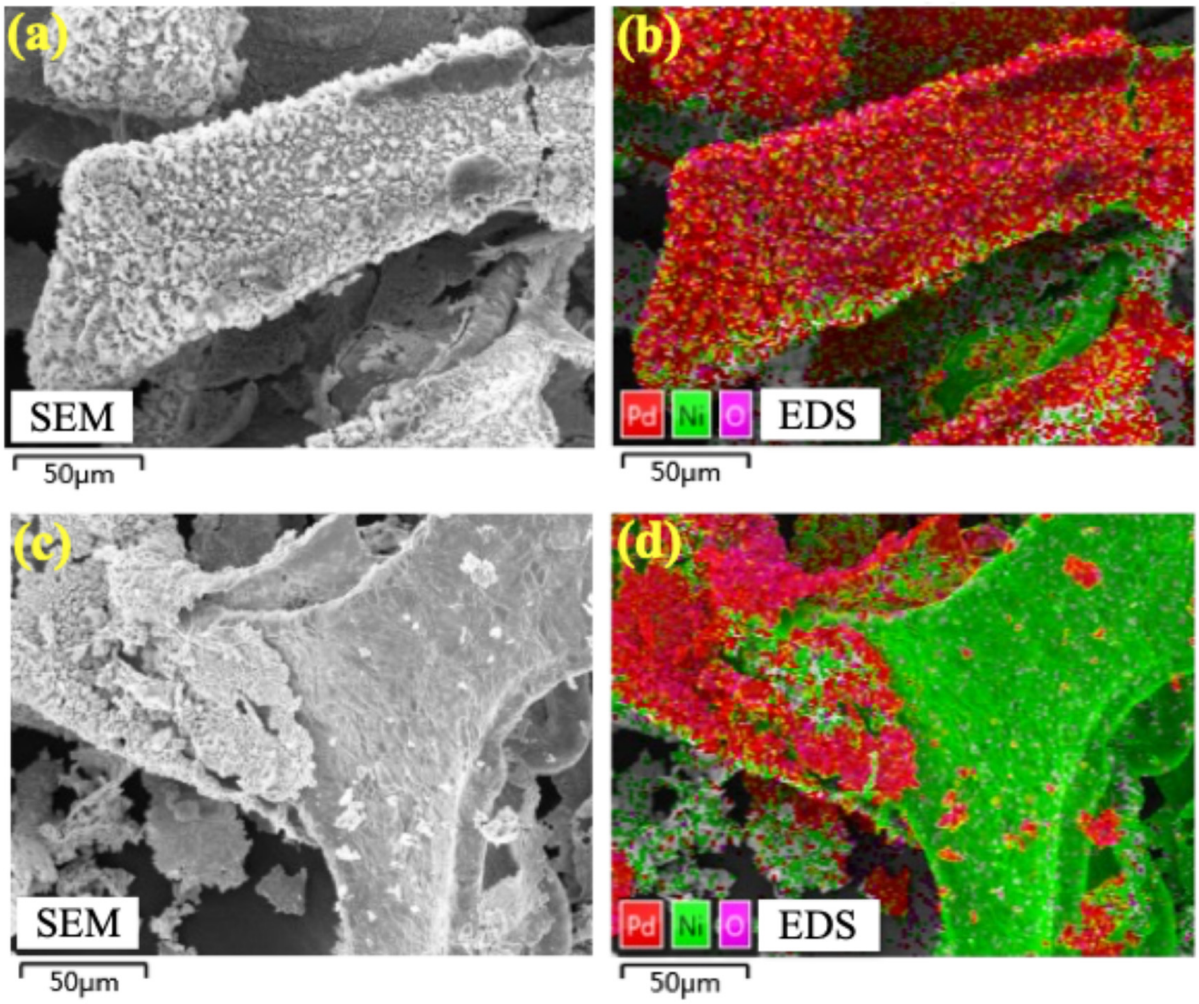


Figure 10. SEM and EDS of 15.16%Pd/Ni foam before and after four cycles of experiments. (**a**,**c**) The SEM of 15.16%Pd/Ni foam before and after four cycles of experiments. (**b**,**d**) The EDS of the distributions of 15.16%Pd/Ni foam before and after four cycles of experiments.

4. Conclusions

In conclusion, this study systematically investigated the electrochemical reduction debromination performance of polybrominated diphenyl ethers (PBDEs) using Pd/Ni, Pd/Cu, and Pd/Ag foams as catalytic electrodes. The results demonstrate that the loading of Pd significantly enhances the catalytic reduction debromination performance of the three electrode materials on BDE-47, with 15.16%Pd/Ni foam showing the most pronounced improvement, followed by 9.37%Pd/Cu and 10.26%Pd/Ag. An analysis of the primary reduction products of BDE-47 reveals that the degradation mechanism for Pd/Ni and Pd/Ag materials is predominantly governed by the active hydrogen atom transfer mechanism, while for the Pd/Cu material, the electron transfer mechanism plays a dominant role. Comparing the debromination efficiency of the reduction products, the Pd/Ni foam electrode exhibits the highest debromination capability. Subsequently, the 15.16%Pd/Ni foam, which demonstrated the best degradation performance, was selected to further investigate the effects of the electrolyte, current density, and the degree of bromination of PBDEs. The results indicate that the presence of an electrolyte significantly inhibits the degradation of BDE-47. The degradation rate of BDE-47 initially increases with the current density, reaches its peak efficiency at 4 mA, and then declines as the current density continues to rise. Moreover, 15.16%Pd/Ni foam exhibits effective degradation performance across PBDEs with varying degrees of bromination, underscoring its broad applicability and versatility. The cycling experiments further demonstrated the declining performance of the 15.16%Pd/Ni foam electrode, with degradation efficiency decreasing from 94.3% in the first cycle to 56.58% in the fourth cycle. The Pd loss and structural damage caused by hydrogen embrittlement and acidic corrosion were identified as key factors limiting the material's long-term stability. To enhance the practical application of Pd/Ni foam electrodes, future studies should focus on reducing Pd loss, improving the stability of the Ni material, minimizing hydrogen-induced embrittlement, and optimizing the reaction conditions to extend the electrode's lifespan. Overall, the findings provide valuable insights into the development of efficient and sustainable catalytic materials for the electrochemical degradation of PBDEs, while offering preliminary evidence of its potential adaptability to other structural-like persistent organic pollutants such as polybrominated biphenyls.

Supplementary Materials: The following supporting information can be downloaded at: https://www.mdpi.com/article/10.3390/pr13030853/s1, Table S1: Theoretical Pd loading ratios of Ni, Cu, and Ag foam electrodes; Figure S1: Debromination pathways of BDE-47; Figure S2: Generation of lower brominated products from BDE-47 with Pd/Ni foam of different Pd loadings; Figure S3: Generation of lower brominated products from BDE-47 with Pd/Cu foam of different Pd loadings; Figure S4: Generation of lower brominated products from BDE-47 with Pd/Ag foam of different Pd loadings.

Author Contributions: Writing—original draft preparation, C.L.; writing—review and editing, H.L., J.L., X.D. and G.L.; Investigation, C.L., H.L. and X.T. All authors have read and agreed to the published version of the manuscript.

Funding: This research was funded by the National Natural Science Foundation of China (Nos. 42077114 and 42277380) and the Local Innovation and Entrepreneurship Team Project of Guangdong Special Support Program (No. 2019BT02L218).

Data Availability Statement: The data presented in this study are available on request from the corresponding author due to the copyright of our experimental data.

Acknowledgments: The authors are grateful to the Ecological Restoration Research Group for their support in PBDEs' degradation experiments.

Conflicts of Interest: The authors declare no conflicts of interest.

References

1. Abbasi, G.; Li, L.; Breivik, K. Global Historical Stocks and Emissions of PBDEs. *Environ. Sci. Technol.* **2019**, *53*, 6330–6340. [CrossRef] [PubMed]
2. Anh, H.Q.; Nam, V.D.; Tri, T.M.; Ha, N.M.; Ngoc, N.T.; Mai, P.T.N.; Anh, D.H.; Minh, N.H.; Tuan, N.A.; Minh, T.B. Polybrominated Diphenyl Ethers in Plastic Products, Indoor Dust, Sediment and Fish from Informal e-Waste Recycling Sites in Vietnam: A Comprehensive Assessment of Contamination, Accumulation Pattern, Emissions, and Human Exposure. *Environ. Geochem. Health* **2017**, *39*, 935–954. [CrossRef] [PubMed]
3. Wang, R.; Cheng, H.; Bian, Z. Global Occurrence and Environmental Behavior of Novel Brominated Flame Retardants in Soils: Current Knowledge and Future Perspectives. *J. Hazard. Mater.* **2024**, *480*, 136298. [CrossRef]
4. Sharkey, M.; Harrad, S.; Abou-Elwafa Abdallah, M.; Drage, D.S.; Berresheim, H. Phasing-out of Legacy Brominated Flame Retardants: The UNEP Stockholm Convention and Other Legislative Action Worldwide. *Environ. Int.* **2020**, *144*, 106041. [CrossRef]
5. Labunska, I.; Harrad, S.; Wang, M.; Santillo, D.; Johnston, P. Human Dietary Exposure to PBDEs Around E-Waste Recycling Sites in Eastern China. *Environ. Sci. Technol.* **2014**, *48*, 5555–5564. [CrossRef]
6. Liang, J.; Wang, R.; Liu, H.; Xie, D.; Tao, X.; Zhou, J.; Yin, H.; Dang, Z.; Lu, G. Unintentional Formation of Mixed Chloro-Bromo Diphenyl Ethers (PBCDEs), Dibenzo-p-Dioxins and Dibenzofurans (PBCDD/Fs) from Pyrolysis of Polybrominated Diphenyl Ethers (PBDEs). *Chemosphere* **2022**, *308*, 136246. [CrossRef]
7. Liang, J.; Lu, G.; Wang, R.; Tang, T.; Huang, K.; Jiang, F.; Yu, W.; Tao, X.; Yin, H.; Dang, Z. The Formation Pathways of Polybrominated Dibenzo-p-Dioxins and Dibenzofurans (PBDD/Fs) from Pyrolysis of Polybrominated Diphenyl Ethers (PBDEs): Effects of Bromination Arrangement and Level. *J. Hazard. Mater.* **2020**, *399*, 123004. [CrossRef] [PubMed]
8. Li, T.-Y.; Zhou, J.-F.; Wu, C.-C.; Bao, L.-J.; Shi, L.; Zeng, E.Y. Characteristics of Polybrominated Diphenyl Ethers Released from Thermal Treatment and Open Burning of E-Waste. *Environ. Sci. Technol.* **2018**, *52*, 4650–4657. [CrossRef]
9. Guo, J.; Zhang, R.; Xu, Z. PBDEs Emission from Waste Printed Wiring Boards during Thermal Process. *Environ. Sci. Technol.* **2015**, *49*, 2716–2723. [CrossRef]
10. Gao, S.; Hong, J.; Yu, Z.; Wang, J.; Yang, G.; Sheng, G.; Fu, J. Polybrominated Diphenyl Ethers in Surface Soils from E-Waste Recycling Areas and Industrial Areas in South China: Concentration Levels, Congener Profile, and Inventory. *Environ. Toxicol. Chem.* **2011**, *30*, 2688–2696. [CrossRef]
11. Li, W.-L.; Ma, W.-L.; Jia, H.-L.; Hong, W.-J.; Moon, H.-B.; Nakata, H.; Minh, N.H.; Sinha, R.K.; Chi, K.H.; Kannan, K.; et al. Polybrominated Diphenyl Ethers (PBDEs) in Surface Soils across Five Asian Countries: Levels, Spatial Distribution, and Source Contribution. *Environ. Sci. Technol.* **2016**, *50*, 12779–12788. [CrossRef] [PubMed]
12. Liu, M.; Huang, B.; Bi, X.; Ren, Z.; Sheng, G.; Fu, J. Heavy Metals and Organic Compounds Contamination in Soil from an E-Waste Region in South China. *Environ. Sci. Process. Impacts* **2013**, *15*, 919. [CrossRef] [PubMed]
13. Tang, X.; Zeng, B.; Hashmi, M.Z.; Long, D.; Yu, B.; Ullah, N.; Shen, C.; Chen, Y. PBDEs and PCDD/Fs in Surface Soil Taken from the Taizhou e-Waste Recycling Area, China. *Chem. Ecol.* **2014**, *30*, 245–251. [CrossRef]
14. Zhang, S.; Xu, X.; Wu, Y.; Ge, J.; Li, W.; Huo, X. Polybrominated Diphenyl Ethers in Residential and Agricultural Soils from an Electronic Waste Polluted Region in South China: Distribution, Compositional Profile, and Sources. *Chemosphere* **2014**, *102*, 55–60. [CrossRef]
15. Huang, Y.; Zhang, D.; Yang, Y.; Zeng, X.; Ran, Y. Distribution and Partitioning of Polybrominated Diphenyl Ethers in Sediments from the Pearl River Delta and Guiyu, South China. *Environ. Pollut.* **2018**, *235*, 104–112. [CrossRef]
16. Alabi, O.A.; Bakare, A.A.; Xu, X.; Li, B.; Zhang, Y.; Huo, X. Comparative Evaluation of Environmental Contamination and DNA Damage Induced by Electronic-Waste in Nigeria and China. *Sci. Total Environ.* **2012**, *423*, 62–72. [CrossRef]
17. Labunska, I.; Harrad, S.; Santillo, D.; Johnston, P.; Brigden, K. Levels and Distribution of Polybrominated Diphenyl Ethers in Soil, Sediment and Dust Samples Collected from Various Electronic Waste Recycling Sites within Guiyu Town, Southern China. *Environ. Sci. Process. Impacts* **2013**, *15*, 503. [CrossRef]
18. Ling, S.; Zhou, S.; Tan, J.; Lu, C.; Fu, M.; Peng, C.; Zhang, W.; Hu, S.; Lin, K.; Zhou, B. Brominated Flame Retardants (BFRs) in Sediment from a Typical e-Waste Dismantling Region in Southern China: Occurrence, Spatial Distribution, Composition Profiles, and Ecological Risks. *Sci. Total Environ.* **2022**, *824*, 153813. [CrossRef]
19. Yu, K.; Gu, C.; Boyd, S.A.; Liu, C.; Sun, C.; Teppen, B.J.; Li, H. Rapid and Extensive Debromination of Decabromodiphenyl Ether by Smectite Clay-Templated Subnanoscale Zero-Valent Iron. *Environ. Sci. Technol.* **2012**, *46*, 8969–8975. [CrossRef]
20. Su, J.; Lu, N.; Zhao, J.; Yu, H.; Huang, H.; Dong, X.; Quan, X. Nano-Cubic Structured Titanium Nitride Particle Films as Cathodes for the Effective Electrocatalytic Debromination of BDE-47. *J. Hazard. Mater.* **2012**, *231–232*, 105–113. [CrossRef]
21. Wang, R.; Tang, T.; Lu, G.; Huang, K.; Yin, H.; Lin, Z.; Wu, F.; Dang, Z. Rapid Debromination of Polybrominated Diphenyl Ethers (PBDEs) by Zero Valent Metal and Bimetals: Mechanisms and Pathways Assisted by Density Function Theory Calculation. *Environ. Pollut.* **2018**, *240*, 745–753. [CrossRef] [PubMed]

22. Tang, T.; Lu, G.; Wang, R.; Chen, H.; Fang, Y.; Huang, K.; Zheng, J.; Zou, M.; Tao, X.; Yin, H.; et al. Debromination of Polybrominated Diphenyl Ethers (PBDEs) by Zero Valent Zinc: Mechanisms and Predicting Descriptors. *J. Hazard. Mater.* **2018**, *352*, 165–171. [CrossRef] [PubMed]
23. Wang, R.; Lu, G.; Lin, H.; Huang, K.; Tang, T.; Xue, X.; Yang, X.; Yin, H.; Dang, Z. Relative Roles of H-Atom Transfer and Electron Transfer in the Debromination of Polybrominated Diphenyl Ethers by Palladized Nanoscale Zerovalent Iron. *Environ. Pollut.* **2017**, *222*, 331–337. [CrossRef]
24. Lei, M.; Wang, N.; Zhu, L.; Tang, H. Peculiar and Rapid Photocatalytic Degradation of Tetrabromodiphenyl Ethers over Ag/TiO_2 Induced by Interaction between Silver Nanoparticles and Bromine Atoms in the Target. *Chemosphere* **2016**, *150*, 536–544. [CrossRef] [PubMed]
25. Shi, J.; Qu, R.; Feng, M.; Wang, X.; Wang, L.; Yang, S.; Wang, Z. Oxidative Degradation of Decabromodiphenyl Ether (BDE 209) by Potassium Permanganate: Reaction Pathways, Kinetics, and Mechanisms Assisted by Density Functional Theory Calculations. *Environ. Sci. Technol.* **2015**, *49*, 4209–4217. [CrossRef]
26. Liang, J.; Liu, H.; Zou, M.; Tao, X.; Zhou, J.; Dang, Z.; Lu, G. Degradation Efficiency and Mechanism of 2,2′,4,4′-Tetrabromodiphenyl Ether (BDE-47) by Thermally Activated Persulfate System. *Chemosphere* **2023**, *325*, 138396. [CrossRef] [PubMed]
27. Luo, S.; Yang, S.; Sun, C.; Gu, J.-D. Improved Debromination of Polybrominated Diphenyl Ethers by Bimetallic Iron–Silver Nanoparticles Coupled with Microwave Energy. *Sci. Total Environ.* **2012**, *429*, 300–308. [CrossRef]
28. Li, L.; Chang, W.; Wang, Y.; Ji, H.; Chen, C.; Ma, W.; Zhao, J. Rapid, Photocatalytic, and Deep Debromination of Polybrominated Diphenyl Ethers on Pd–TiO_2: Intermediates and Pathways. *Chem. Eur. J.* **2014**, *20*, 11163–11170. [CrossRef]
29. Du, X.; Li, H.; Liang, J.; Wang, R.; Huang, K.; Hayat, W.; Cai, L.; Tao, X.; Dang, Z.; Lu, G. Hydrogen-Donor-Controlled Polybrominated Dibenzofuran (PBDF) Formation from Polybrominated Diphenyl Ether (PBDE) Photolysis in Solutions: Competition Mechanisms of Radical-Based Cyclization and Hydrogen Abstraction Reactions. *Environ. Sci. Technol.* **2023**, *57*, 7777–7788. [CrossRef]
30. Konstantinov, A.; Bejan, D.; Bunce, N.J.; Chittim, B.; McCrindle, R.; Potter, D.; Tashiro, C. Electrolytic Debromination of PBDEs in DE-83TM Technical Decabromodiphenyl Ether. *Chemosphere* **2008**, *72*, 1159–1162. [CrossRef]
31. Peverly, A.A.; Pasciak, E.M.; Strawsine, L.M.; Wagoner, E.R.; Peters, D.G. Electrochemical Reduction of Decabromodiphenyl Ether at Carbon and Silver Cathodes in Dimethylformamide and Dimethyl Sulfoxide. *J. Electroanal. Chem.* **2013**, *704*, 227–232. [CrossRef]
32. Aguiar, T.; Baumann, L.; Albuquerque, A.; Teixeira, L.; De Souza Gil, E.; Scalize, P. Application of Electrocoagulation for the Removal of Transition Metals in Water. *Sustainability* **2023**, *15*, 1492. [CrossRef]
33. Cao, S.; Huang, H.; Shi, K.; Wei, L.; You, N.; Fan, X.; Yang, Z.; Zhang, W. Engineering Superhydrophilic/Superaerophobic Hierarchical Structures of Co-CH@NiFe-LDH/NF to Boost the Oxygen Evolution Reaction. *Chem. Eng. J.* **2021**, *422*, 130123. [CrossRef]
34. Qu, C.; Soomro, G.S.; Ren, N.; Liang, D.; Lu, S.; Xiang, Y.; Zhang, S. Enhanced Electro-Oxidation/Peroxone (In Situ) Process with a Ti-Based Nickel-Antimony Doped Tin Oxide Anode for Phenol Degradation. *J. Hazard. Mater.* **2020**, *384*, 121398. [CrossRef]
35. Xiong, M.; Chen, W.; Gu, S.; Zhang, D.; Ma, C.; Gu, H.; Meng, Y.; Jin, Y.; Xu, Z. Core-Shell Structured Fe/Ni@C Ternary Micro-Electrolysis Material for 4-Nitrochlorobenzen Removal: Performance Assessment and Mechanism Insight. *J. Clean. Prod.* **2022**, *372*, 133769. [CrossRef]
36. Tri, D.V.; Anh, N.T.; Luu, T.L.; Trippel, J.; Wagner, M. Electrochemical Degradation of Perfluorooctanoic Acid (PFOA) and Perfluorooctane Sulfonate (PFOS) in Water with Persulfate Catalyst Support. *Sep. Purif. Technol.* **2025**, *363*, 132076. [CrossRef]
37. Vanrenterghem, B.; Papaderakis, A.; Sotiropoulos, S.; Tsiplakides, D.; Balomenou, S.; Bals, S.; Breugelmans, T. The Reduction of Benzylbromide at Ag-Ni Deposits Prepared by Galvanic Replacement. *Electrochim. Acta* **2016**, *196*, 756–768. [CrossRef]
38. Zheng, Z.; Lu, G.; Wang, R.; Huang, K.; Tao, X.; Yang, Y.; Zou, M.; Xie, Y.; Yin, H.; Shi, Z.; et al. Effects of Surfactant on the Degradation of 2,2′,4,4′-Tetrabromodiphenyl Ether (BDE-47) by Nanoscale Ag/Fe Particles: Kinetics, Mechanisms and Intermediates. *Environ. Pollut.* **2019**, *245*, 780–788. [CrossRef]
39. Zhuang, Y.; Ahn, S.; Seyfferth, A.L.; Masue-Slowey, Y.; Fendorf, S.; Luthy, R.G. Dehalogenation of Polybrominated Diphenyl Ethers and Polychlorinated Biphenyl by Bimetallic, Impregnated, and Nanoscale Zerovalent Iron. *Environ. Sci. Technol.* **2011**, *45*, 4896–4903. [CrossRef] [PubMed]
40. Wang, R.; Tang, T.; Wei, Y.; Dang, D.; Huang, K.; Chen, X.; Yin, H.; Tao, X.; Lin, Z.; Dang, Z.; et al. Photocatalytic Debromination of Polybrominated Diphenyl Ethers (PBDEs) on Metal Doped TiO2 Nanocomposites: Mechanisms and Pathways. *Environ. Int.* **2019**, *127*, 5–12. [CrossRef] [PubMed]
41. Shen, Y.; Tong, Y.; Xu, J.; Wang, S.; Wang, J.; Zeng, T.; He, Z.; Yang, W.; Song, S. Ni-Based Layered Metal-Organic Frameworks with Palladium for Electrochemical Dechlorination. *Appl. Catal. B Environ.* **2020**, *264*, 118505. [CrossRef]

42. Li, J.; Luan, C.; Cui, Y.; Zhang, H.; Wang, L.; Wang, H.; Zhang, Z.; Zhao, B.; Zhang, H.; Zhang, X.; et al. Preparation and Characterization of Palladium/Polyaniline/Foamed Nickel Composite Electrode for Electrocatalytic Dechlorination. *Sep. Purif. Technol.* **2019**, *211*, 198–206. [CrossRef]
43. Sun, Z.; Wei, X.; Hu, X.; Wang, K.; Shen, H. Electrocatalytic Dechlorination of 2,4-Dichlorophenol in Aqueous Solution on Palladium Loaded Meshed Titanium Electrode Modified with Polymeric Pyrrole and Surfactant. *Colloids Surf. Physicochem. Eng. Asp.* **2012**, *414*, 314–319. [CrossRef]
44. Fan, J.; Du, H.; Zhao, Y.; Wang, Q.; Liu, Y.; Li, D.; Feng, J. Recent Progress on Rational Design of Bimetallic Pd Based Catalysts and Their Advanced Catalysis. *ACS Catal.* **2020**, *10*, 13560–13583. [CrossRef]
45. Bagger, A.; Ju, W.; Varela, A.S.; Strasser, P.; Rossmeisl, J. Electrochemical CO_2 Reduction: A Classification Problem. *ChemPhysChem* **2017**, *18*, 3266–3273. [CrossRef]
46. Wu, J.; Shan, S.; Luo, J.; Joseph, P.; Petkov, V.; Zhong, C.-J. PdCu Nanoalloy Electrocatalysts in Oxygen Reduction Reaction: Role of Composition and Phase State in Catalytic Synergy. *ACS Appl. Mater. Interfaces* **2015**, *7*, 25906–25913. [CrossRef]
47. Wu, Y.; Huo, X.; Zhang, W. Synergistic Pd/Cu Catalysis in Organic Synthesis. *Chem. Eur. J.* **2020**, *26*, 4895–4916. [CrossRef]
48. Neukermans, S.; Vorobjov, F.; Kenis, T.; De Wolf, R.; Hereijgers, J.; Breugelmans, T. Electrochemical Reduction of Halogenated Aromatic Compounds at Metal Cathodes in Acetonitrile. *Electrochim. Acta* **2020**, *332*, 135484. [CrossRef]
49. Guo, S.; Zhu, L.; Majima, T.; Lei, M.; Tang, H. Reductive Debromination of Polybrominated Diphenyl Ethers: Dependence on Br Number of the Br-Rich Phenyl Ring. *Environ. Sci. Technol.* **2019**, *53*, 4433–4439. [CrossRef]
50. Boucher, B.A.; Ennis, J.K.; Tsirlin, D.; Harris, S.A. A Global Database of Polybrominated Diphenyl Ether Flame Retardant Congeners in Foods and Supplements. *J. Food Compos. Anal.* **2018**, *69*, 171–188. [CrossRef]
51. Lee, H.J.; Kim, G.B. An Overview of Polybrominated Diphenyl Ethers (PBDEs) in the Marine Environment. *Ocean Sci. J.* **2015**, *50*, 119–142. [CrossRef]
52. Deng, C.; Chen, Y.; Li, J.; Li, Y.; Li, H. Environmental Pollution of Polybrominated Diphenyl Ethers from Industrial Plants in China: A Preliminary Investigation. *Environ. Sci. Pollut. Res.* **2016**, *23*, 7012–7021. [CrossRef]

Disclaimer/Publisher's Note: The statements, opinions and data contained in all publications are solely those of the individual author(s) and contributor(s) and not of MDPI and/or the editor(s). MDPI and/or the editor(s) disclaim responsibility for any injury to people or property resulting from any ideas, methods, instructions or products referred to in the content.